

Evidence for freeze-out of charge fluctuations in the quark-gluon plasma at the LHC

Jonathan Parra,¹ Roman Poberezhniuk,^{1,2} Volker Koch,³ Claudia Ratti,¹ and Volodymyr Vovchenko¹

¹Physics Department, University of Houston, Box 351550, Houston, TX 77204, USA

²Bogolyubov Institute for Theoretical Physics, 03680 Kyiv, Ukraine

³Nuclear Science Division, Lawrence Berkeley National Laboratory, 1 Cyclotron Road, Berkeley, CA 94720, USA

The D-measure of event-by-event net-charge fluctuations was introduced over 20 years ago as a potential signal of quark-gluon plasma (QGP) in heavy-ion collisions, where it is expected to be suppressed due to the fractional electric charges of quarks. Measurements have been performed at RHIC and LHC, but the conclusion has been elusive in the absence of quantitative calculations for both scenarios. We address this issue by employing a recently developed formalism of density correlations and incorporate resonance decays, local charge conservation, and experimental kinematic cuts. We find that the hadron gas scenario is in fair agreement with the ALICE data for $\sqrt{s_{\text{NN}}} = 2.76$ TeV Pb–Pb collisions only when a very short rapidity range of local charge conservation is enforced, while the QGP scenario is in excellent agreement with experimental data and largely insensitive to the range of local charge conservation. A Bayesian analysis of the data utilizing different priors yields moderate evidence for the freeze-out of charge fluctuations in the QGP phase relative to hadron gas. The upcoming high-fidelity measurements from LHC Run 2 will serve as a precision test of the two scenarios.

Introduction.— Heavy-ion collisions at ultrarelativistic energies provide a unique environment for studying matter under extreme conditions, where the formation of the quark–gluon plasma (QGP) is expected to occur. From first-principles lattice QCD calculations, it is now understood that the deconfinement transition is a smooth crossover at LHC energies [1]. Numerous measurements at the LHC and RHIC have provided evidence for the creation of a hot and strongly interacting medium consistent with QGP formation [2–8] (see Ref. [9] for a recent overview). Event-by-event net-charge fluctuations can serve as a distinct QGP signal due to their sensitivity to the relevant degrees of freedom in the medium [10, 11]. In particular, the D-measure of net-charge fluctuations,

$$D = 4 \frac{\kappa_2[Q]}{\langle N_{\text{ch}} \rangle}, \quad (1)$$

was introduced to quantify the anticipated suppression of fluctuations arising from the fractional charges of quarks in a deconfined phase [11]. Here, $Q = N_+ - N_-$ is the net charge [12], N_{\pm} are multiplicities of positively and negatively charged particles, $N_{\text{ch}} = N_+ + N_-$ is the total charged particle multiplicity, $\langle \dots \rangle$ denotes event-by-event averaging, and $\kappa_2[Q] = \langle Q^2 \rangle - \langle Q \rangle^2$ is the variance of net-charge distribution.

Since quarks carry fractional charges, the D-measure is expected to be significantly smaller in the QGP. For a pion gas in the grand-canonical ensemble (GCE), one has $D_{\pi} \approx 4$ reflecting their unit charge and Poisson statistics, while a smaller value of $D_{\text{HG}} \approx 3$ is expected in a hadron gas (HG) due to resonance decays. Obtaining the estimate for QGP is less straightforward, mainly because $\langle N_{\text{ch}} \rangle$ is not defined in the QGP phase. The estimates based on entropy conservation and values of charge susceptibility in QGP yield $D_{\text{QGP}} \approx 1$, about three times smaller than the hadron gas value.

The above estimates correspond to the GCE limit. However, the measurements in heavy-ion collisions are subject to kinematic cuts. Furthermore, the measurements are affected by the exact (local) conservation of electric charge [13–15] and diffusive dynamics [16, 17]. For this reason, the analysis of experimental measurements of the D-measure by STAR [18, 19] and ALICE [20], which tend to lie in-between the naive GCE estimates for HG and QGP, has been inconclusive. Kinematic cuts and global charge conservation have been considered in hadronic gas calculations [13, 21], but this has not been sufficient to describe the data. The D-measure has been calculated using microscopic transport models at LHC [22] and RHIC [23, 24] energies, and its connection to charge balance functions [25, 26] has also been explored [27]. However, drawing definitive conclusions remains challenging due to the lack of quantitative modeling of HG and QGP scenarios on an equal footing.

In this Letter, we present quantitative calculations for both the HG and QGP scenarios for Pb–Pb collisions at LHC energies. First, we revisit the estimates for the normalized charge fluctuation $\omega = \kappa_2[Q]/\langle N_{\text{ch}}^{\text{prim}} \rangle$ at hadronization, which is expressed in terms of charge susceptibility χ_2^Q and entropy density s at the stage where charge fluctuations freeze out and distinguish HG and QGP scenarios. We then incorporate the effect of resonance decays, local charge fluctuations, and kinematic cuts through the use of the 2-point charge density correlator within a recently developed framework [28]. We perform a Bayesian analysis of experimental data of the ALICE Collaboration for Pb–Pb collisions at $\sqrt{s_{\text{NN}}} = 2.76$ TeV and obtain moderate evidence for freeze-out in the QGP. We argue that the upcoming high-statistics data from LHC Run 2 will provide a precision test of these scenarios.

Fluctuations at hadronization.— The starting point of our analysis is the hadronization stage. We study the fol-

lowing scenario. The mean charged multiplicity $\langle N_{\text{ch}}^{\text{prim}} \rangle$ is in chemical equilibrium and determined by the Hadron Resonance Gas (HRG) model, carrying no memory of QGP. However, the net-charge variance, $\kappa_2[Q]$, may freeze out earlier than the mean multiplicities, possibly in the QGP phase. We quantify charge fluctuations at hadronization through

$$\omega = \frac{\kappa_2[Q]}{\langle N_{\text{ch}}^{\text{prim}} \rangle}. \quad (2)$$

Here $\kappa_2[Q]$ is the charge variance and $\langle N_{\text{ch}}^{\text{prim}} \rangle$ the multiplicity of charged hadrons at hadronization, i.e. before resonance decays. We assume the GCE for the time being. If fluctuations freeze out in the hadron gas, one expects the Poisson baseline of $\omega_{\text{HG}} \approx 1$. A quantitative calculation within the HRG model [29] gives a slightly larger value, $\omega_{\text{HG}} \approx 1.1$ at $T = 155 - 160$ MeV, with the enhancement attributed to the Bose-Einstein statistics for pions and the presence of multi-charged hadrons.

Estimating ω for the QGP phase is more tricky, as $\langle N_{\text{ch}}^{\text{prim}} \rangle$ is not well-defined outside the hadronic phase. One thus typically resorts to using the entropy density s as a proxy [3, 10, 11], utilizing the approximately isentropic evolution between the freeze-out of charge fluctuations and hadronization. In the grand-canonical ensemble, the charge susceptibility is a measure of net-charge variance per unit volume, thus $\kappa_2[Q] = V\chi_2^Q$. Dividing and multiplying ω by the entropy S and then by the final charged multiplicity $\langle N_{\text{ch}} \rangle$ one can write

$$\begin{aligned} \omega &= \frac{\kappa_2[Q]}{\langle N_{\text{ch}}^{\text{prim}} \rangle} = \frac{V\chi_2^Q}{S} \frac{S}{\langle N_{\text{ch}}^{\text{prim}} \rangle} \\ &= \frac{\chi_2^Q}{s} \frac{S}{\langle N_{\text{ch}} \rangle} \frac{\langle N_{\text{ch}} \rangle}{\langle N_{\text{ch}}^{\text{prim}} \rangle}. \end{aligned} \quad (3)$$

Here the charge susceptibility χ_2^Q and entropy density s are given by the equation of state, such as the free (Stefan-Boltzmann) QGP limit or lattice QCD [30]. $S/\langle N_{\text{ch}} \rangle$ is the entropy per charged hadron in the final state. While earlier estimates for $S/\langle N_{\text{ch}} \rangle$ had varied significantly, recent studies at LHC energies give the value $S/\langle N_{\text{ch}} \rangle = 6.7 \pm 0.8$ [31] which we employ here. The last term is the ratio $\langle N_{\text{ch}} \rangle / \langle N_{\text{ch}}^{\text{prim}} \rangle$ of the final and primordial charged multiplicities, which is enhanced relative to unity by resonance decays. A thermal model estimate at $T = 155$ MeV gives $\gamma_Q = \langle N_{\text{ch}} \rangle / \langle N_{\text{ch}}^{\text{prim}} \rangle \approx 1.67$ [29]. For a free gas of massless u, d, s -quarks and gluons one has $(\chi_2^Q)_{\text{QGP}}/T^3 = 2/3$ and $s_{\text{QGP}}/T^3 = 19\pi^2/9$, therefore

$$\omega_{\text{QGP}} = 0.36 \pm 0.04. \quad (4)$$

The uncertainty here comes solely from $S/\langle N_{\text{ch}} \rangle$.

Equation (3) defines the value of ω in a more general case beyond just HG and QGP limits. In particular, one can utilize lattice QCD data for χ_2^Q and s/T^3 to evaluate ω

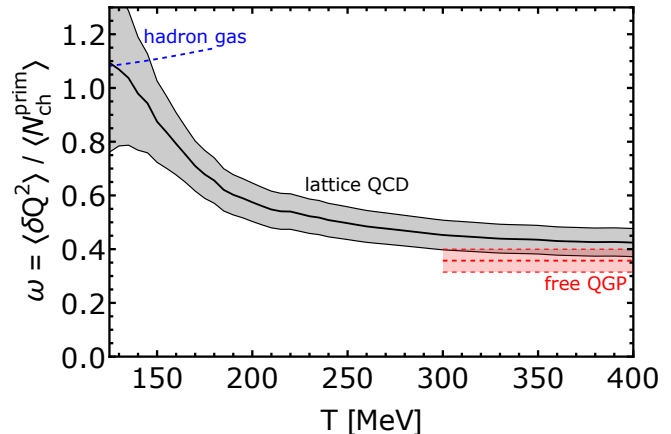


Figure 1. Temperature dependence of the normalized charge variance $\omega = \kappa_2[Q]/\langle N_{\text{ch}}^{\text{prim}} \rangle$ computed through Eq. (3) using lattice QCD data for χ_2^Q and s/T^3 (gray band), as well as the hadron resonance gas (dashed blue line) and free massless QGP (dashed red line) limits. The error bands reflect the uncertainties in lattice QCD data [32, 33] and $S/\langle N_{\text{ch}} \rangle$ [31].

for a freeze-out of charge fluctuations at a particular temperature. The corresponding temperature dependence of ω is depicted in Fig. 1, utilizing the lattice QCD data of the Wuppertal–Budapest collaboration [32, 33]. The lattice-based results indicate that ω smoothly evolves from the hadron gas regime at $T \lesssim 160$ MeV ($\omega \simeq 1.1$) to the QGP regime at higher temperature, with $\omega \approx 0.40 - 0.45$ at $T \geq 300$ MeV close to the Stefan-Boltzmann limit of $\omega_{\text{QGP}} \simeq 0.36$. If ω can be reliably extracted from the data, one could map it to the temperature at which the freeze-out of charge fluctuations occurs.

Charge susceptibility and resonance decays.— By construction, the charge susceptibility at hadronization is $\chi_2^Q = \omega \langle n_{\text{ch}}^{\text{prim}} \rangle$ where $\langle n_{\text{ch}}^{\text{prim}} \rangle$ is the charged particle density. One can decompose χ_2^Q as follows:

$$\chi_2^Q = \langle n_{\text{ch}}^{\text{prim}} \rangle + \varphi_2^{Q,\text{prim}}. \quad (5)$$

The first term — $\langle n_{\text{ch}}^{\text{prim}} \rangle$ — is the Skellam distribution baseline corresponding to the uncorrelated production of charged hadrons. This term is also referred to as self-correlation [27, 34]. The second term — $\varphi_2^{Q,\text{prim}}$ — describes correlations among the produced charges at hadronization. Given that $\chi_2^Q = \omega \langle n_{\text{ch}}^{\text{prim}} \rangle$, one has

$$\varphi_2^{Q,\text{prim}} = (\omega - 1) \langle n_{\text{ch}}^{\text{prim}} \rangle. \quad (6)$$

A value of ω different from unity implies the presence of (anti-)correlations among charges at hadronization. In particular, the QGP scenario where $\omega \approx 0.36$ implies a significant anti-correlation among charges.

Resonance decays during the hadronic phase produce additional correlations among final charged particles. The most prominent such example is the $\rho^0 \rightarrow \pi^+\pi^-$ decay,

which introduces a correlation between positively and negatively charged pions. We incorporate this effect in the following way. As the electric charge is conserved in all resonance decays, the full charge susceptibility χ_2^Q does not change. However, decays increase the final charged particle multiplicity, $\langle n_{\text{ch}} \rangle = \gamma_Q \langle n_{\text{ch}}^{\text{prim}} \rangle$, leading to a rebalancing between the contributions from the self-correlation and two-particle correlations to χ_2^Q . The parameter $\gamma_Q = \langle n_{\text{ch}} \rangle / \langle n_{\text{ch}}^{\text{prim}} \rangle$ has been introduced in Eq. (3) above and we employ the thermal model estimate $\gamma_Q \simeq 1.67$ throughout. Writing the final charged susceptibility as

$$\chi_2^Q = \langle n_{\text{ch}} \rangle + \varphi_2^Q \quad (7)$$

and using $\chi_2^Q = \omega \langle n_{\text{ch}}^{\text{prim}} \rangle$ and $\langle n_{\text{ch}} \rangle = \gamma_Q \langle n_{\text{ch}}^{\text{prim}} \rangle$ one obtains:

$$\varphi_2^Q = \left(\frac{\omega}{\gamma_Q} - 1 \right) \langle n_{\text{ch}} \rangle. \quad (8)$$

One can see that resonance decays ($\gamma_Q > 1$) introduce the additional anti-correlations among charges in the final state.

2-point correlator and exact charge conservation.— To account for collective flow, charge conservation, and kinematical cuts, we employ a differential 2-point charge correlator,

$$\mathcal{C}_2^Q(\mathbf{r}_1, \mathbf{r}_2) \equiv \langle \delta\rho_Q(\mathbf{r}_1) \delta\rho_Q(\mathbf{r}_2) \rangle, \quad (9)$$

where $\delta\rho_Q(\mathbf{r}_i) = \rho_Q(\mathbf{r}_i) - \langle \rho_Q(\mathbf{r}_i) \rangle$ is the net-charge density fluctuation at coordinate \mathbf{r}_i . Integrating $\mathcal{C}_2^Q(\mathbf{r}_1, \mathbf{r}_2)$ over a particular subvolume produces the variance of net-charge distribution of particles emitted from that sub-volume. In a recent work [28], the 2-point correlator $\mathcal{C}_2^Q(\mathbf{r}_1, \mathbf{r}_2)$ was derived for a thermal system with local charge conservation:

$$\mathcal{C}_2^Q(\mathbf{r}_1, \mathbf{r}_2) = \chi_2^Q \left[\delta(\mathbf{r}_1 - \mathbf{r}_2) - \frac{\varkappa(\mathbf{r}_1, \mathbf{r}_2)}{V_{\text{tot}}} \right]. \quad (10)$$

Here χ_2^Q is the grand-canonical charge susceptibility, $V_{\text{tot}} = \int d\mathbf{r}$ is the total system volume, and $\varkappa(\mathbf{r}_1, \mathbf{r}_2)$ corresponds to exact charge conservation over the full fireball volume. This last quantity satisfies the sum rule $\int d\mathbf{r}_{1,2} \varkappa(\mathbf{r}_1, \mathbf{r}_2) = 1$. In global equilibrium (global charge conservation only) $\varkappa(\mathbf{r}_1, \mathbf{r}_2) = 1$ while local charge conservation can be modeled by $\varkappa(\mathbf{r}_1, \mathbf{r}_2)$ which is peaked at small relative distance between \mathbf{r}_1 and \mathbf{r}_2 .

At LHC, we integrate over the transverse plane and consider only the longitudinal (spatial) rapidity coordinate, $\mathbf{r} \rightarrow \eta$. We assume that the net-charge susceptibility χ_2^Q is independent of η , but we do allow for a non-uniform distribution in η of the system volume, characterized by volume rapidity density $\rho_V(\eta) = dV/d\eta(\eta)$. In this case, the volume element reads $d\mathbf{r} = \rho_V(\eta)d\eta$ and $d\mathbf{r}_1 d\mathbf{r}_2 \delta(\mathbf{r}_1 - \mathbf{r}_2) = d\eta_1 d\eta_2 \rho_V(\eta_1) \delta(\eta_1 - \eta_2)$.

Therefore, the two-point correlator in spatial rapidity reads

$$\begin{aligned} \mathcal{C}_2^Q(\eta_1, \eta_2) &= \rho_V(\eta_1) \chi_2^Q \left[\delta(\eta_1 - \eta_2) - \rho_V(\eta_2) \frac{\varkappa(\eta_1, \eta_2)}{V_{\text{tot}}} \right] \\ &= \rho_V(\eta_1) \langle n_{\text{ch}} \rangle \delta(\eta_1 - \eta_2) \\ &\quad + \rho_V(\eta_1) \left(\frac{\omega}{\gamma_Q} - 1 \right) \langle n_{\text{ch}} \rangle \delta(\eta_1 - \eta_2) \\ &\quad - \rho_V(\eta_1) \rho_V(\eta_2) \frac{\omega}{\gamma_Q} \langle n_{\text{ch}} \rangle \frac{\varkappa(\eta_1, \eta_2)}{V_{\text{tot}}}. \quad (11) \end{aligned}$$

Here, the first term corresponds to self-correlation, the second term describes local two-particle correlations, such as due to ρ^0 decays or hadronization of QGP, and the last term corresponds to non-local two-particle correlations due to exact charge conservation.

For the volume rapidity density, we considered a uniform (boost-invariant) profile, $\rho_V(\eta) \propto \frac{\theta(\eta_{\text{max}} - |\eta|)}{2\eta_{\text{max}}}$ and a Gaussian volume distribution, $\rho_V(\eta) \propto \exp\left(-\frac{\eta^2}{2\sigma_V^2}\right)$. The parameters η_{max} and σ_V are fixed through the measurements [35, 36] of the rapidity density of charged multiplicity [21]. We find the differences between the two scenarios for the charge fluctuations measured at midrapidity to be virtually negligible and thus focus on the uniform volume distribution in the following.

Local charge conservation.— Local charge conservation is modeled by a Gaussian profile, as studied [15] and motivated by balance function measurements [37–39]:

$$\varkappa(\eta_1, \eta_2) \propto \exp\left[-\frac{(\eta_1 - \eta_2)^2}{2\sigma_y^2}\right], \quad (12)$$

where σ_y quantifies the range of local charge conservation in spatial rapidity. For convenience, we will use the size of the effective conservation volume V_c relative to the total volume V_{tot} to quantify local charge conservation. This ratio is given by [15]

$$\frac{V_c}{V_{\text{tot}}} = \sqrt{\frac{\pi}{2}} \frac{\sigma_y}{\eta_{\text{max}}} \text{erf}\left(\frac{\eta_{\text{max}}}{\sqrt{2}\sigma_y}\right). \quad (13)$$

Note that $V_c \rightarrow V_{\text{tot}}$ as $\sigma_y \rightarrow \infty$, as expected for the global charge conservation limit. We treat the ratio V_c/V_{tot} as a free parameter in this study.

Kinematic cuts.— To account for collective flow and experimental cuts in momentum, we employ the binomial model for acceptance probability, following Ref. [28]. Specifically, we assume that a final charged particle with spatial rapidity η ultimately has momentum acceptance probability $p(\eta)$ that is independent of the other particles. The variance of net charge in momentum acceptance is then obtained by folding the integration of $\mathcal{C}_2^Q(\eta_1, \eta_2)$ over spatial rapidities with the binomial distribution at each (η_1, η_2) pair. The self-correlation term in the 2-point correlator \mathcal{C}_2^Q in Eq. (11) is diluted by a factor $p(\eta_1)$, while the

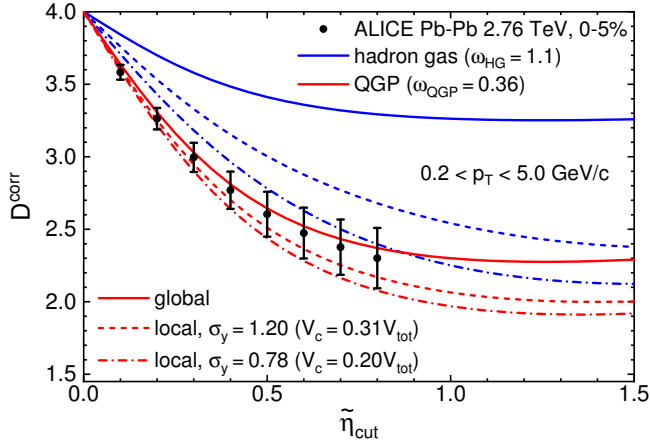


Figure 2. The corrected D-measure as a function of pseudorapidity cut $\tilde{\eta}_{\text{cut}}$ in central Pb–Pb collisions at $\sqrt{s_{\text{NN}}} = 2.76$ TeV calculated via Eq. (17) for hadron gas (blue lines) and QGP (red lines) scenarios with global (solid lines) and local (styled lines) charge conservation. The symbols depict the experimental data of the ALICE Collaboration [20].

other terms correspond to two-particle correlations and are diluted by a factor $p(\eta_1)p(\eta_2)$, leading to

$$\begin{aligned} \kappa_2[Q^{\text{acc}}] = & V_{\text{tot}} \langle n_{\text{ch}} \rangle \left[\langle p(\eta) \rangle - \left(1 - \frac{\omega}{\gamma_Q} \right) \langle p^2(\eta) \rangle \right. \\ & \left. - \frac{\omega}{\gamma_Q} \langle p(\eta_1)p(\eta_2) \rangle_{\neq} \right]. \end{aligned} \quad (14)$$

Here,

$$\langle p^n(\eta) \rangle = \frac{1}{2\eta_{\text{max}}} \int d\eta p^n(\eta), \quad (15)$$

$$\langle p(\eta_1)p(\eta_2) \rangle_{\neq} = \frac{1}{4\eta_{\text{max}}^2} \iint d\eta_1 d\eta_2 p(\eta_1)p(\eta_2) \neq(\eta_1, \eta_2). \quad (16)$$

The mean acceptance probability $\langle p(\eta) \rangle$ also determines the mean charged multiplicity inside the acceptance, $\langle N_{\text{ch}}^{\text{acc}} \rangle = V_{\text{tot}} \langle n_{\text{ch}} \rangle \langle p(\eta) \rangle$. Therefore, the D-measure inside momentum acceptance $D = 4\kappa_2[Q^{\text{acc}}] / \langle N_{\text{ch}}^{\text{acc}} \rangle$ reads

$$D = 4 \left\{ 1 - \left(1 - \frac{\omega}{\gamma_Q} \right) \frac{\langle p^2(\eta) \rangle}{\langle p(\eta) \rangle} - \frac{\omega}{\gamma_Q} \frac{\langle p(\eta_1)p(\eta_2) \rangle_{\neq}}{\langle p(\eta) \rangle} \right\}. \quad (17)$$

Equation (17) is the central technical result of this Letter. It quantifies the contributions of the self-correlation (first term), local two-particle correlations (second term), and non-local two-particle correlations (third term) to the final result, arising from the simultaneous effects of the possible early freeze-out of fluctuations (ω), resonance decays (γ_Q), local charge conservation (\neq), collective flow and kinematic cuts $[p(\eta)]$.

Comparison with experimental data.— The ALICE Collaboration reported measuring the D-measure in Pb–Pb

collisions at $\sqrt{s_{\text{NN}}} = 2.76$ TeV [20]. The measurements were performed in a broad transverse momentum window, $0.2 < p_T < 5.0$ GeV/c as a function of the pseudorapidity cut $|\tilde{\eta}| < \tilde{\eta}_{\text{cut}}$ (up to $\tilde{\eta}_{\text{cut}} = 0.8$). We take $\gamma_Q = 1.67$ and contrast hadron gas ($\omega_{\text{HG}} = 1.1$) and QGP ($\omega_{\text{QGP}} = 0.36$) scenarios. To elucidate the effect of local charge conservation, we performed the calculations for global charge conservation ($V_c = V_{\text{tot}}$), and two values of local charge conservation, $V_c = 0.2V_{\text{tot}}$ ($\sigma_y = 0.78$) and $V_c = 0.31V_{\text{tot}}$ ($\sigma_y = 1.20$) which are motivated by analyzing local baryon conservation in Ref. [28]. We use the blast-wave model [40] to evaluate acceptance probabilities $p(\eta)$, with the parameters taken from [41]. We compute $p(\eta)$ as a weighted average of acceptance probabilities for pions, kaons, and protons, based on their relative measured yields. Finally, we note that the measurements in [20] are corrected for global charge conservation, namely $D^{\text{corr}} = (D' + D'')/2$, where $D' = D + 4\langle p(\eta) \rangle$ and $D'' = \frac{D}{1 - \langle p(\eta) \rangle}$. We perform the same correction for comparisons with data.

Figure 2 compares our model calculations for D^{corr} with the experimental data. The hadron gas scenario with only global charge conservation fails to describe the data (solid blue line). The result is consistent with prior studies [21]. A more reasonable agreement is obtained if significant local conservation is enforced, $\sigma_y = 0.78$ (dash-dotted blue line). In contrast, the QGP scenario exhibits much weaker sensitivity to local charge conservation, and a fair agreement with experimental data is obtained for almost any value of V_c . This weak sensitivity is attributed to the fact that the local conservation term [Eq. (17)] is proportional to ω , which is more than three times smaller in QGP relative to HG.

Bayesian analysis.— Our result generally indicates the preference for the QGP scenario, although the HG scenario may also be feasible for a sufficiently local range of charge conservation. Thus, the conclusion may be sensitive to the prior assumption on the range of local charge conservation. In addition to the two extreme scenarios considered above, it is also feasible to explore the freeze-out of fluctuations at an intermediate stage between QGP and HG. To further investigate this, we perform a Bayesian analysis of experimental data in the $(\omega, V_c/V_{\text{tot}})$ parameter space, utilizing the Gaussian likelihood function. The experimental uncertainties for different data points are expected to be correlated, given that the data points correspond to overlapping acceptances. We thus only include the smallest $\tilde{\eta}_{\text{cut}} = 0.1$ and largest $\tilde{\eta}_{\text{cut}} = 0.8$ acceptance data points into the likelihood, for which we can neglect the correlation.

The parameter ω is varied in the range $\omega \in [0, 1.2]$. In this way, one covers both the HG and QGP scenarios, as well as intermediate values and even an extreme case of vanishing local fluctuations ($\omega \rightarrow 0$). We adopt a uniform prior throughout, $\omega \sim U(0, 1.2)$, which attributes equal prior probability for HG and QGP. The conservation volume is varied in the range $V_c/V_{\text{tot}} \in [0, 1]$, which

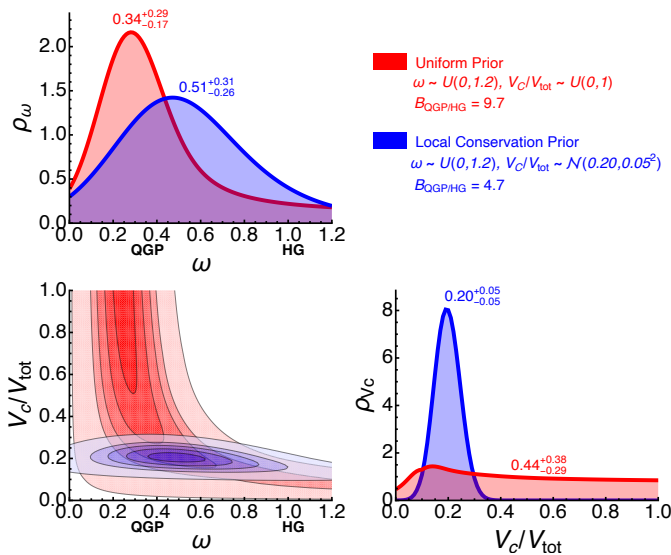


Figure 3. Posterior distribution for ω and V_c/V_{tot} obtained from our Bayesian analysis of $\sqrt{s_{\text{NN}}} = 2.76$ TeV data employing uniform (red) and local conservation (blue) priors. The labels indicate the 68% confidence interval around the median. The contours in the lower left plot represent 10%, 30%, 50%, 68%, and 95% confidence regions for the joint $(\omega, V_c/V_{\text{tot}})$ distribution.

covers both the highly local and fully global charge conservation range. We consider two scenarios for the prior distribution: (i) uniform prior, $V_c/V_{\text{tot}} \sim U(0, 1)$, and (ii) a prior preferring local charge conservation, modeled by a Gaussian distribution in V_c/V_{tot} with the mean value of 0.20 and standard deviation of 0.05, i.e. $V_c/V_{\text{tot}} \sim \mathcal{N}(0.20, 0.05^2)$. These values are motivated by the analysis of net-proton cumulants in Ref. [28].

The posterior distributions are shown in Fig. 3. For both scenarios, one observes only minor changes in the posterior distribution of V_c in comparison to the prior, indicating that the D-measure is not very sensitive to V_c . One exception would be if the prior distribution for ω was strongly biased toward the HG scenario, as in this case, only a highly local V_c could reasonably describe the data. The posterior distribution for ω is more interesting. For a uniform V_c prior, one observes a considerable preference for QGP, with $\omega_{\text{CI}}^{68\%} = 0.34^{+0.28}_{-0.16}$. Contrasting QGP ($\omega_{\text{QGP}} = 0.36$) and HG ($\omega_{\text{HG}} = 1.1$) scenarios via the Bayes factor, one obtains $B_{\text{QGP}/\text{HG}} = 9.7$ indicating moderate evidence (bordering strong evidence) according to Jeffreys' classification scale [42, 43]. Giving a strong prior preference to a local charge conservation leads to $\omega_{\text{CI}}^{68\%} = 0.53^{+0.30}_{-0.27}$ and $B_{\text{QGP}/\text{HG}} = 4.7$ which still indicates moderate (but close to anecdotal) evidence for QGP.

Predictions for 5.02 TeV.— The upcoming high-statistics measurements at $\sqrt{s_{\text{NN}}} = 5.02$ TeV from the ALICE and CMS experiments [44] during LHC Run 2 are expected to have notably reduced error bars and, thus, greater constraining power. We performed calculations for the HG

and QGP scenarios in central Pb–Pb collisions at $\sqrt{s_{\text{NN}}} = 5.02$ TeV utilizing the newly developed framework. The difference relative to the $\sqrt{s_{\text{NN}}} = 2.76$ TeV case comes from a larger spatial rapidity coverage ($\eta_{\text{max}} = 5.1$) and slightly modified blast-wave parameters [45]. The results are qualitatively the same as those shown in Fig. 2. For completeness, we present quantitative calculations for different kinematic acceptances in the supplemental material. We note that a sizable portion of experimental error at $\sqrt{s_{\text{NN}}} = 2.76$ TeV comes from the difference between the D' and D'' corrections. Given that our calculations already incorporate local charge conservation, we advocate for a direct analysis of the uncorrected D-measure in Run 2 to enhance discriminating power.

Summary and outlook.— We developed a new formalism for analyzing net-charge fluctuations in heavy-ion collisions, which allowed us to calculate the D-measure with the simultaneous treatment of the suppression of fluctuations due to QGP, correlations from resonance decays, local charge conservation, collective flow, and momentum acceptance. We find that the hadron gas scenario is in fair agreement with the ALICE data for $\sqrt{s_{\text{NN}}} = 2.76$ TeV Pb–Pb collisions only when a very short rapidity range of local charge conservation is enforced, while the QGP scenario is in excellent agreement with experimental data and largely insensitive to the range of local charge conservation. A Bayesian data analysis reveals moderate evidence for the freeze-out of charge fluctuations in the QGP phase. The two scenarios can be tested further with the upcoming high-precision data from LHC Run 2. The formalism offers ample opportunity for extensions, including the application to finite baryon densities and RHIC energies, hadronic phase dynamics, variation of priors, the analysis of high-order fluctuations, and balance functions.

Acknowledgments. V.V. thanks Mesut Arslanok for the fruitful discussions. This work was supported by the U.S. Department of Energy, Office of Science, Office of Nuclear Physics, under contract numbers DE-SC0022023 (J.P., C.R., V.V.) and DE-AC02-05CH11231 (V.K.). This material is based upon work supported by the National Science Foundation under grants No. PHY-2208724 and PHY-2116686, and within the framework of the MUSES collaboration, under Grant No. OAC-2103680.

- [1] Y. Aoki, G. Endrodi, Z. Fodor, S. D. Katz, and K. K. Szabo, *Nature* **443**, 675 (2006), arXiv:hep-lat/0611014.
- [2] J. W. Harris and B. Muller, *Ann. Rev. Nucl. Part. Sci.* **46**, 71 (1996), arXiv:hep-ph/9602235.
- [3] S. A. Bass, M. Gyulassy, H. Stoecker, and W. Greiner, *J. Phys. G* **25**, R1 (1999), arXiv:hep-ph/9810281.
- [4] I. Arsene *et al.* (BRAHMS), *Nucl. Phys. A* **757**, 1 (2005), arXiv:nucl-ex/0410020.
- [5] B. B. Back *et al.* (PHOBOS), *Nucl. Phys. A* **757**, 28 (2005), arXiv:nucl-ex/0410022.

- [6] J. Adams *et al.* (STAR), *Nucl. Phys. A* **757**, 102 (2005), [arXiv:nucl-ex/0501009](#).
- [7] K. Adcox *et al.* (PHENIX), *Nucl. Phys. A* **757**, 184 (2005), [arXiv:nucl-ex/0410003](#).
- [8] S. Acharya *et al.* (ALICE), *Eur. Phys. J. C* **84**, 813 (2024), [arXiv:2211.04384 \[nucl-ex\]](#).
- [9] J. W. Harris and B. Müller, *Eur. Phys. J. C* **84**, 247 (2024), [arXiv:2308.05743 \[hep-ph\]](#).
- [10] M. Asakawa, U. W. Heinz, and B. Müller, *Phys. Rev. Lett.* **85**, 2072 (2000), [arXiv:hep-ph/0003169](#).
- [11] S. Jeon and V. Koch, *Phys. Rev. Lett.* **85**, 2076 (2000), [arXiv:hep-ph/0003168](#).
- [12] We neglect multi-charged hadrons in the final state such as light nuclei.
- [13] M. Bleicher, S. Jeon, and V. Koch, *Phys. Rev. C* **62**, 061902 (2000), [arXiv:hep-ph/0006201](#).
- [14] M. Sakaida, M. Asakawa, and M. Kitazawa, *Phys. Rev. C* **90**, 064911 (2014), [arXiv:1409.6866 \[nucl-th\]](#).
- [15] V. Vovchenko, O. Savchuk, R. V. Poberezhnyuk, M. I. Gorenstein, and V. Koch, *Phys. Lett. B* **811**, 135868 (2020), [arXiv:2003.13905 \[hep-ph\]](#).
- [16] E. V. Shuryak and M. A. Stephanov, *Phys. Rev. C* **63**, 064903 (2001), [arXiv:hep-ph/0010100](#).
- [17] M. A. Aziz and S. Gavin, *Phys. Rev. C* **70**, 034905 (2004), [arXiv:nucl-th/0404058](#).
- [18] J. Adams *et al.* (STAR), *Phys. Rev. C* **68**, 044905 (2003), [arXiv:nucl-ex/0307007](#).
- [19] B. I. Abelev *et al.* (STAR), *Phys. Rev. C* **79**, 024906 (2009), [arXiv:0807.3269 \[nucl-ex\]](#).
- [20] B. Abelev *et al.* (ALICE), *Phys. Rev. Lett.* **110**, 152301 (2013), [arXiv:1207.6068 \[nucl-ex\]](#).
- [21] V. Vovchenko and V. Koch, *Phys. Rev. C* **103**, 044903 (2021), [arXiv:2012.09954 \[hep-ph\]](#).
- [22] D. K. Mishra, P. K. Netrakanti, and P. Garg, *Phys. Rev. C* **95**, 054905 (2017), [arXiv:1705.04440 \[nucl-th\]](#).
- [23] Q. H. Zhang, V. Topor Pop, S. Jeon, and C. Gale, *Phys. Rev. C* **66**, 014909 (2002), [arXiv:hep-ph/0202057](#).
- [24] V. K. Singh, D. K. Mishra, and Z. Ahammed, *Phys. Rev. C* **101**, 014903 (2020), [arXiv:1907.02850 \[hep-ph\]](#).
- [25] S. A. Bass, P. Danielewicz, and S. Pratt, *Phys. Rev. Lett.* **85**, 2689 (2000), [arXiv:nucl-th/0005044](#).
- [26] S. Pratt and C. Plumberg, *Phys. Rev. C* **104**, 014906 (2021), [arXiv:2104.00628 \[nucl-th\]](#).
- [27] B. Ling, T. Springer, and M. Stephanov, *Phys. Rev. C* **89**, 064901 (2014), [arXiv:1310.6036 \[nucl-th\]](#).
- [28] V. Vovchenko, *Phys. Rev. C* **110**, L061902 (2024), [arXiv:2409.01397 \[hep-ph\]](#).
- [29] V. Vovchenko and H. Stoecker, *Comput. Phys. Commun.* **244**, 295 (2019), [arXiv:1901.05249 \[nucl-th\]](#).
- [30] In lattice QCD one commonly uses dimensionless charge susceptibility $\tilde{\chi}_2^Q$, which differs from the one used here by factor T^3 , namely $\tilde{\chi}_2^Q = \chi_2^Q/T^3$.
- [31] P. Hanus, A. Mazeliauskas, and K. Reyers, *Phys. Rev. C* **100**, 064903 (2019), [arXiv:1908.02792 \[hep-ph\]](#).
- [32] S. Borsanyi, Z. Fodor, S. D. Katz, S. Krieg, C. Ratti, and K. Szabo, *JHEP* **01**, 138, [arXiv:1112.4416 \[hep-lat\]](#).
- [33] S. Borsanyi, Z. Fodor, C. Hoelbling, S. D. Katz, S. Krieg, and K. K. Szabo, *Phys. Lett. B* **730**, 99 (2014), [arXiv:1309.5258 \[hep-lat\]](#).
- [34] S. Pratt, *Phys. Rev. Lett.* **108**, 212301 (2012), [arXiv:1203.4578 \[nucl-th\]](#).
- [35] E. Abbas *et al.* (ALICE), *Phys. Lett. B* **726**, 610 (2013), [arXiv:1304.0347 \[nucl-ex\]](#).
- [36] J. Adam *et al.* (ALICE), *Phys. Lett. B* **772**, 567 (2017), [arXiv:1612.08966 \[nucl-ex\]](#).
- [37] J. Adams *et al.* (STAR), *Phys. Rev. Lett.* **90**, 172301 (2003), [arXiv:nucl-ex/0301014](#).
- [38] B. Abelev *et al.* (ALICE), *Phys. Lett. B* **723**, 267 (2013), [arXiv:1301.3756 \[nucl-ex\]](#).
- [39] S. Acharya *et al.* (ALICE), *Phys. Lett. B* **833**, 137338 (2022), [arXiv:2110.06566 \[nucl-ex\]](#).
- [40] E. Schnedermann, J. Sollfrank, and U. W. Heinz, *Phys. Rev. C* **48**, 2462 (1993), [arXiv:nucl-th/9307020](#).
- [41] B. Abelev *et al.* (ALICE), *Phys. Rev. C* **88**, 044910 (2013), [arXiv:1303.0737 \[hep-ex\]](#).
- [42] H. Jeffreys, *The Theory of Probability*, 3rd ed. (Oxford University Press, 1961).
- [43] M. D. Lee and E.-J. Wagenmakers, *Bayesian Cognitive Modeling: A Practical Course* (Cambridge University Press, 2014).
- [44] CMS Physics Analysis Note “Net-charge fluctuations in PbPb collisions at 5.02 TeV” (2023).
- [45] S. Acharya *et al.* (ALICE), *Phys. Rev. C* **101**, 044907 (2020), [arXiv:1910.07678 \[nucl-ex\]](#).

Supplemental material

Blast-wave model

We calculate the charge acceptance probability $p(\eta)$ emitted from spatial rapidity η as a weighted sum of pion, kaon, and proton contributions,

$$p(\eta) = w_\pi p_\pi(\eta) + w_K p_K(\eta) + w_p p_p(\eta) \quad (\text{A.1})$$

where the weights $w_\pi = 0.84$, $w_K = 0.12$, and $w_p = 0.04$ correspond to the relative midrapidity yields dN/dy for pions, kaons, and protons measured by the ALICE Collaboration in 0-5% Pb–Pb collisions at $\sqrt{s_{\text{NN}}} = 2.76$ TeV [41]. For $\sqrt{s_{\text{NN}}} = 5.02$ TeV, the corresponding values are $w_\pi = 0.83$, $w_K = 0.13$, and $w_p = 0.04$ [45].

To calculate the acceptance probability $p_i(\eta)$ for a single particle species we use the blast-wave model [40] which incorporates the presence of longitudinal and radial collective flow. The momentum distribution of a single particle emitted

from spatial rapidity η within the blast-wave model is given by

$$\frac{d^3 N_i}{p_T dp_T dy}(\eta) \propto m_T \cosh(y - \eta) \int_0^1 \zeta d\zeta \exp \left[-\frac{m_T \cosh \rho \cosh(y - \eta)}{T_{\text{kin}}} \right] I_0 \left(\frac{p_T \sinh \rho}{T_{\text{kin}}} \right), \quad (\text{A.2})$$

where $\zeta \in [0, 1]$ is the normalized radial coordinate in the transverse plane, $\rho = \tanh^{-1}(\beta_s \zeta^{n_{\text{bw}}})$ denotes the transverse flow rapidity, y is the momentum rapidity, and T_{kin} is the kinetic freeze-out temperature of the system. The transverse mass is defined as $m_T = \sqrt{p_T^2 + m_i^2}$ with $m_\pi \approx 138$ MeV, $m_K \approx 494$ MeV, and $m_p \approx 938$ MeV. The surface transverse velocity β_s and the blast wave exponent n_{bw} control the maximum transverse velocity and the shape of the transverse flow velocity profile, respectively. We take the blast-wave parameters $T_{\text{kin}} = 95$ MeV, $\beta_s = 0.883$, and $n_{\text{bw}} = 0.712$ from [41] for 0-5% Pb–Pb collisions at $\sqrt{s_{\text{NN}}} = 2.76$ TeV and for 0-5% Pb–Pb collisions at $\sqrt{s_{\text{NN}}} = 5.02$ TeV we take $T_{\text{kin}} = 90$ MeV, $\beta_s = 0.906$, and $n_{\text{bw}} = 0.735$ from [45].

The D-measure measurements incorporate cuts in transverse momentum, $p_T^{\text{min}} < p_T < p_T^{\text{max}}$, and pseudorapidity, $|\tilde{\eta}| < \tilde{\eta}_{\text{cut}}$. One can map the distribution (A.2) from momentum rapidity y to pseudorapidity $\tilde{\eta}$ through the variable change

$$\sinh y = \frac{p_T}{m_T} \sinh \tilde{\eta}, \quad dy = \frac{p_T \cosh \tilde{\eta}}{\sqrt{(p_T \cosh \tilde{\eta})^2 + m^2}} d\tilde{\eta}, \quad (\text{A.3})$$

giving

$$\frac{d^3 N_i}{dp_T d\tilde{\eta}}(\eta) = \frac{E(\tilde{\eta}, \eta) p_T^2 \cosh \tilde{\eta}}{\sqrt{(p_T \cosh \tilde{\eta})^2 + m^2}} \int_0^1 \zeta d\zeta \exp \left[-\frac{E(\tilde{\eta}, \eta) \cosh \rho}{T_{\text{kin}}} \right] I_0 \left(\frac{p_T \sinh \rho}{T_{\text{kin}}} \right) \quad (\text{A.4})$$

where

$$E(\tilde{\eta}, \eta) \equiv m_T \cosh(y - \eta) = m_T \cosh \left(\text{arcsinh} \left[\frac{p_T \sinh \tilde{\eta}}{m_T} \right] - \eta \right). \quad (\text{A.5})$$

The acceptance probability is calculated as

$$p_i(\eta) = \frac{\int_{p_T^{\text{min}}}^{p_T^{\text{max}}} dp_T \int_{-\tilde{\eta}_{\text{cut}}}^{\tilde{\eta}_{\text{cut}}} d\tilde{\eta} \frac{d^3 N}{dp_T d\tilde{\eta}}(\eta)}{\int_0^\infty dp_T \int_{-\infty}^\infty d\tilde{\eta} \frac{d^3 N}{dp_T d\tilde{\eta}}(\eta)}. \quad (\text{A.6})$$

Here $p_T^{\text{min}} = 0.2$ GeV, $p_T^{\text{max}} = 5$ GeV and $0.1 < \tilde{\eta}_{\text{cut}} < 0.8$ for 2.76 TeV data of ALICE [20]. We evaluate the integrals in (A.6) using Gauss-Kronrod quadrature for each value of η and construct interpolating functions $p_i(\eta)$ for each acceptance cut under consideration. We then use it to calculate the average acceptance probabilities $\langle p(\eta) \rangle$, $\langle p^2(\eta) \rangle$, and $\langle p(\eta_1) p(\eta_2) \rangle$.

LHC Run 2 predictions.

Here we present predictions for the D-measure in central Pb–Pb collisions at $\sqrt{s_{\text{NN}}} = 5.02$ TeV from LHC Run 2. The planned measurements by ALICE are performed in acceptance ranges $0.2(0.6) < p_T < 2.0(5.0)$ GeV/ c at 0-5% centrality as a function of pseudorapidity cut $\tilde{\eta}_{\text{cut}}$. Measurements at CMS are expected to extend acceptance coverage up to $\tilde{\eta}_{\text{cut}}^{\text{max}} = 2$ [44]. Figure A.1 depicts our predictions for the $\tilde{\eta}_{\text{cut}}$ dependence of D-measure for the four p_T ranges. We present our predictions for the uncorrected D-measure, i.e. without the correction for charge conservation, which we argue to be most appropriate for direct comparisons with measurements. One can see that the uncorrected D-measure is notably higher for calculations with $p_T^{\text{min}} = 0.6$ GeV/ c compared to those with $p_T^{\text{min}} = 0.2$ GeV/ c . This reflects stronger effects of charge conservation for a larger acceptance in p_T .

The planned measurements by CMS correspond to 0-5% Pb–Pb collisions with transverse momentum cut $0.5 < p_T < 3.0$ GeV/ c , as a function of pseudorapidity cut up to $\tilde{\eta}_{\text{cut}} = 2.5$ [44]. We present the corresponding predictions in Fig. A.2.

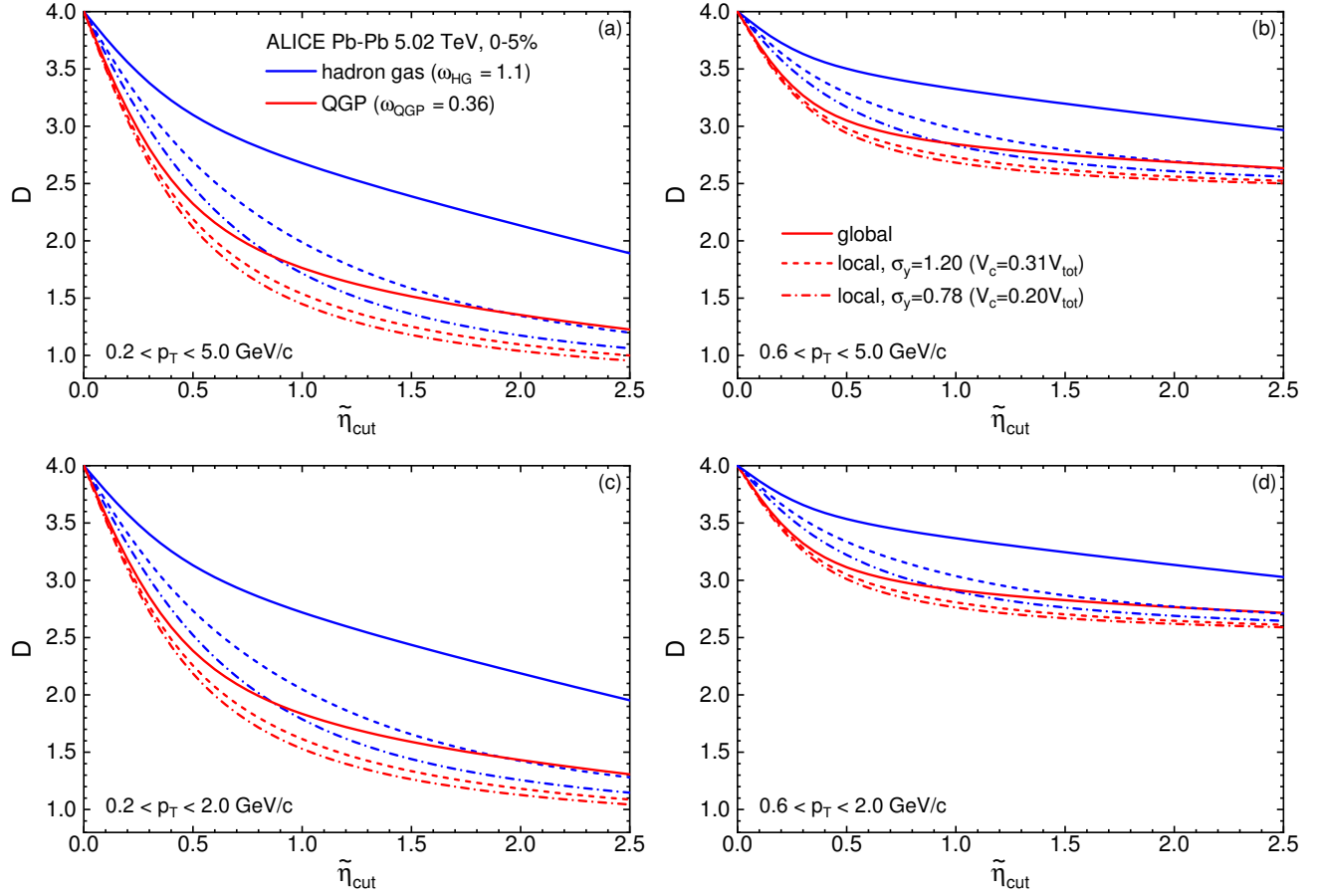


Figure A.1. Predictions for the (uncorrected) D-measure in 0–5% central Pb–Pb collisions at $\sqrt{s_{\text{NN}}} = 5.02$ TeV, plotted as a function of the pseudorapidity acceptance $\tilde{\eta}_{\text{cut}}$ for four different transverse momentum (p_T) ranges analyzed by the ALICE Collaboration. The curves compare the hadron-gas (blue) and QGP (red) freeze-out scenarios under three assumptions about charge conservation: global (solid) and local with two different rapidity ranges, $\sigma_y = 1.20$ (dashed) and $\sigma_y = 0.78$ (dash-dotted).

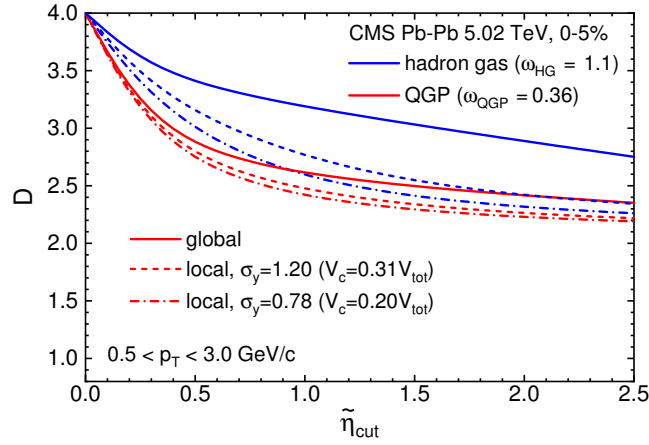


Figure A.2. Same as Fig. A.1 but for transverse momentum range $0.5 < p_T < 3.0$ GeV/c studied by the CMS Collaboration.